Structural and optical properties of erbium-doped Ba 0.7 Sr 0.3 Ti O 3 thin films

Shou-Yi Kuo and Wen-Feng Hsieh

Citation: Journal of Vacuum Science & Technology A **23**, 768 (2005); doi: 10.1116/1.1938979
View online: http://dx.doi.org/10.1116/1.1938979
View Table of Contents: http://scitation.aip.org/content/avs/journal/jvsta/23/4?ver=pdfcov
Published by the AVS: Science & Technology of Materials, Interfaces, and Processing

Structural and optical properties of erbium-doped $Ba_{0.7}Sr_{0.3}TiO_3$ thin films

Shou-Yi Kuo[a)]
Instrument Technology Research Center, National Applied Research Laboratories, Taiwan

Wen-Feng Hsieh
Department of Photonics and Institute of Electro-Optical Engineering, National Chiao-Tung University, Taiwan

(Received 4 October 2004; accepted 25 April 2005; published 23 June 2005)

Er-doped $Ba_{0.7}Sr_{0.3}TiO_3$ (BST:Er) thin films prepared by the sol–gel technique have been investigated by means of x-ray diffraction (XRD), Raman, spectroscopic ellipsometry, Capacitance–voltage, and photoluminescence (PL) measurements. XRD results indicate that the film possess the highest degree of crystallinity at the annealing temperature of 700 °C. The dependence of the refractive index on erbium concentration was also analyzed. In addition, the excitation-dependent PL studies indicate that the green emission peaks do not shift with the change in excitation power, while the integrated intensity increases monotonically with the increase in excitation power. The quenching mechanism of the green emission due to dopant concentrations and annealing temperatures was discussed in detail. All experimental results indicate that BST:Er thin films might be a potential candidate for optoelectronics devices. © *2005 American Vacuum Society.* [DOI: 10.1116/1.1938979]

I. INTRODUCTION

Recently, the study of the luminescent properties of the rare-earth (RE) doped materials is strongly motivated because of their various applications in optoelectronic devices and next-generation flat-panel displays.[1–4] Erbium-doped oxides are of special interest due to their characteristic emission at 1.54 μm, corresponding to minimum loss in the silica-based fiber. Except for the distinguishing feature mentioned above, other Er^{3+} transitions in the blue ($^2H_{9/2}\rightarrow{}^4I_{15/2}$), green ($^4S_{3/2}, ^2H_{11/2}\rightarrow{}^4I_{15/2}$), and red ($^4F_{9/2}\rightarrow{}^4I_{15/2}$) spectral regions were also found to have application potential.[5–8] Due to the 4*f* shell of RE ions being well shielded by the outer electrons, the energy of the transitions is relatively independent of the host matrix and the ambient temperature. Nevertheless, the relative intensity of their photoluminescence, chemical stability, and sensitivity to the operation environments are affected by the nature of the matrix, which will also influence their commercialization. In comparison with the traditional sulfide luminescent phosphors, oxide film phosphors offer potential advantages because of their atmospheric stability, reduced degradation under applied voltages, and anticorrosive properties required for practical use.[9–12] The perovskite $Ba_xSr_{1-x}TiO_3$ (BST) has been attracting much attention because of its unique combination of superior dielectric properties, high permittivity, and low leakage current. In addition, Er^{3+} ions can be readily incorporated into barium titanate to form an extended solid solution.[13,14] Therefore, BST:Er will be a promising candidate for optoelectronic devices.

BST thin films have previously been fabricated by different methods such as metalorganic chemical vapor deposition, molecular beam epitaxy, rf sputtering, thermal evaporation, sol–gel and laser ablation.[15–20] Despite the crystalline quality being inferior to other vacuum deposition techniques, the sol–gel processing is still a relatively easy and economical way for making uniform large size, high quality stoichiometric thin film phosphors. So far, there have been only a few reports on the optical properties of Er^{3+}-doped $Ba_xSr_{1-x}TiO_3$ films. The investigations of the optical properties are important to optimize and improve the performance of devices. In this article, we report and discuss the structural and optical properties in the visible spectral region of sol–gel derived erbium-doped $Ba_{0.7}Sr_{0.3}TiO_3$ thin films. As a consequence, the influence of annealing temperature and dopant concentration can also be investigated.

II. EXPERIMENT

The Er-doped thin films on $Pt/TiO_2/SiO_2/Si$ (100) substrates were prepared by the sol–gel method. The precursor solutions were synthesized using barium acetate, strontium acetate, titanium isopropoxide, and erbium acetate as the starting materials. Barium acetate and strontium acetate with a molar ratio of 7:3 and erbium acetate were dissolved in heated glacial acetic, and an appropriate amount of ethylene glycol was added to stabilize the solution. Then equimolar amounts of titanium isopropoxide were also added into the solution. Finally, formamide was selected as an additive to adjust the solution viscosity in order to reduce the crack of BST:Er thin films.[21] The prepared solution was clear and transparent.

The BST:Er thin films were deposited by spinning the diluted solution at a speed 3000 rpm for 30 s. Each layer of the films was dried at 200 °C for 10 min to dry the gel and then pyrolyzed at 500 °C 30 min in a furnace to remove residual organic compounds, followed by a suitable heating rate to obtain crack-free films. Post-annealing of the

[a)]Author to whom correspondence should be addressed; electronic mail: u8624806@itrc.org.tw

multilayer BST:Er thin films was carried out for 1 h at temperatures ranging from 600 to 900 °C under oxygen atmosphere.

The crystalline structure of the thin films was analyzed by x-ray diffraction (XRD) (Siemens D5005) with Cu Kα radiation. For photoluminescence (PL) and Raman measurements, the 488 nm line of an Ar^+ laser was used as the excitation source. The signal was analyzed using a SPEX 1877C triple spectrograph equipped with a cooled charge coupled device at 140 K. The ellipsometric spectra of the films were measured by the spectroscopic ellipsometer (Sopra) with a fixed incident angle of 75°. The incident light beam is polarized before reflecting from the sample. Then the reflected beam, after passing through an analyzer, is dispersed by a monochromator and detected by a photomultiplier. The wavelength range of our measurement is 300–800 nm with 1 nm steps. Capacitance–voltage ($C-V$) analyses were performed using a HP8142 impedance analyzer.

III. RESULTS AND DISCUSSION

Figure 1(a) shows are the XRD patterns of BST:Er films deposited on $Pt/TiO_2/SiO_2/Si$ substrates at various annealing temperatures of 600–800 °C. The thin films annealed at 600 °C show weak perovskite phases such as (100), (110), (111), and (211). Meanwhile, the secondary phases originating from $(Bs,Sr)_2Ti_2O_5CO_3$ and Er_2O_3 were also found.[22,23] The diffraction lines of $Er_2(Si,Ti)_2O_7$ were recognized when annealing temperatures were above 700 °C.[24–26] It is believed that the secondary phase appeared in the thin films during the process of the high annealing temperature. The results indicate that the films annealed at 700 °C have a single and crystalline perovskite phase, consistent with previous reports.[21,27] The XRD patterns of BST films doped with various Er concentrations are shown in Fig. 1(b). It was found that more erbium incorporated into the BST films, the worse the crystallinity appeared as determined by the full width half maximum of XRD spectra. We might attribute the deterioration to the Er^{3+} substitution in the films.

Figure 2 shows the Raman spectrum of 3 mol % Er^{3+}-doped BST film, annealed at 700 °C, taken at room temperature. From this figure, we found a broadband centered at 260 cm^{-1} corresponds to the $A_1(TO_2)$ phonon mode, a peak at 300 cm^{-1} is attributed to the B_1 and $E(TO+LO)$ modes, and the asymmetric broadband near 520 cm^{-1} corresponds to $E(TO)$ and $A_1(TO_3)$ modes. In addition, the Raman peak at 300 cm^{-1} is specific to the tetragonal phase of the polycrystalline $Ba_xSr_{1-x}TiO_3$.[28] It is known that the Curie temperature T_c linearly increases with Ba concentration. A structural change from centrosymmetric cubic to noncentrosymmetric tetragonal phase is observed at room temperature when $x \sim 0.75$.[28] However, the characteristic Raman peaks persist for all BST:Er films, implying these films are in the tetragonal phase. In order to identify the structural phase, expanded XRD data were investigated as shown in Fig. 2(b). The nondegeneracy of the {200/002} reflection is obvious evidence of the tetragonality, which is consistent with an earlier report.[29]

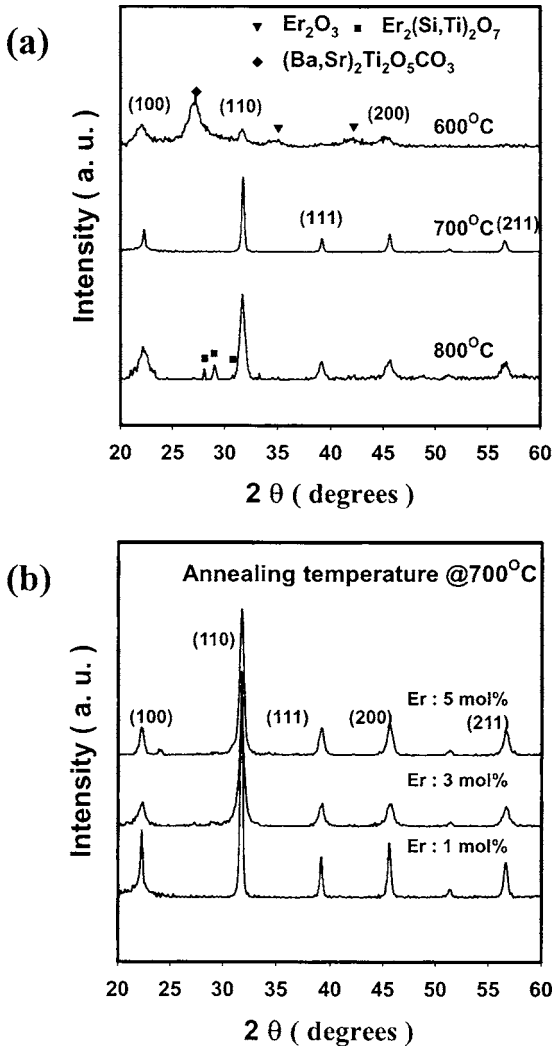

FIG. 1. XRD patterns of BST:Er thin films annealed at various temperatures (a) and doped with various Er concentrations at sintering temperature 700 °C (b). Secondary phases are marked by various symbols.

A Pt top electrode was deposited by rf sputtering for a metal/insulator/metal structure to perform the $C-V$ measurement. The dielectric constants (not shown here) for the 3 mol % doped BST thin film capacitors annealed at different temperatures are 230, 320, and 440 for 600, 700, and 800 °C, respectively. Compared with earlier reports, the results demonstrate that the addition of an Er dopant did not reduce the dielectric properties of BST films.[19,21]

In spectroscopic ellipsometry, one deals with the measurements of the relative changes in the amplitude and phase of a linearly polarized monochromatic incident light upon an oblique reflection from the sample surface. The measured quantities are the traditional ellipsometric angles Ψ and Δ, which are related to the ratio of the complex Fresnel reflection coefficients defined by[30]

$$\rho \equiv \frac{r_p}{r_s} = \tan \Psi \exp(i\Delta), \tag{1}$$

where r_p and r_s are the Fresnel reflection coefficient for light polarized parallel and perpendicular to the plane of inci-

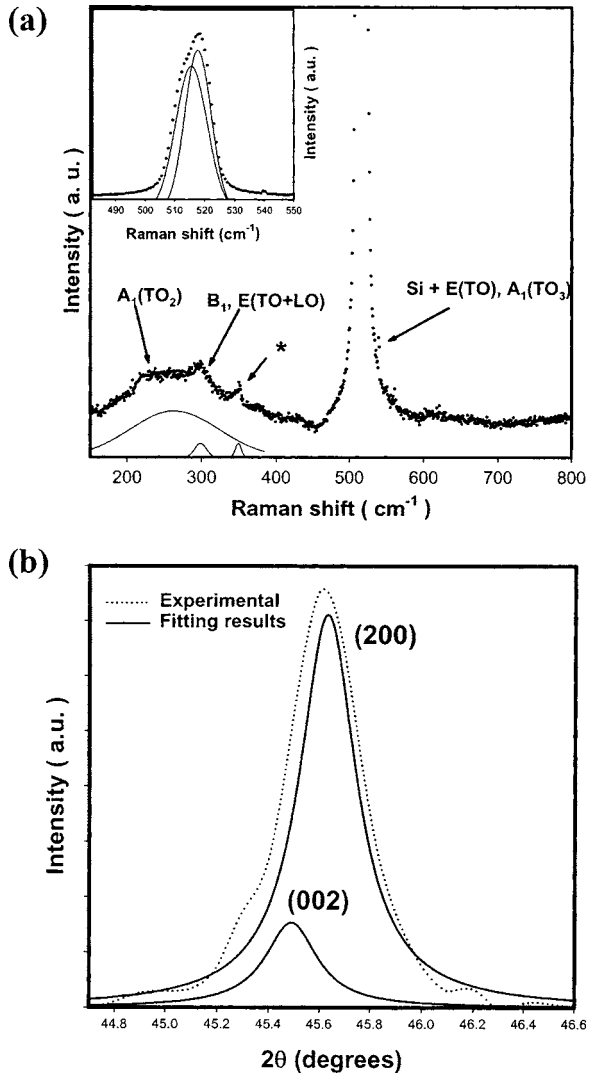

FIG. 2. Raman spectra of BST thin films annealed at temperature 700 °C (a) and typical expanded XRD data around 45.5° (b). An extra peak comes from the laser source and is denoted by (*). The dotted and solid lines represent the experimental and fitting results, respectively.

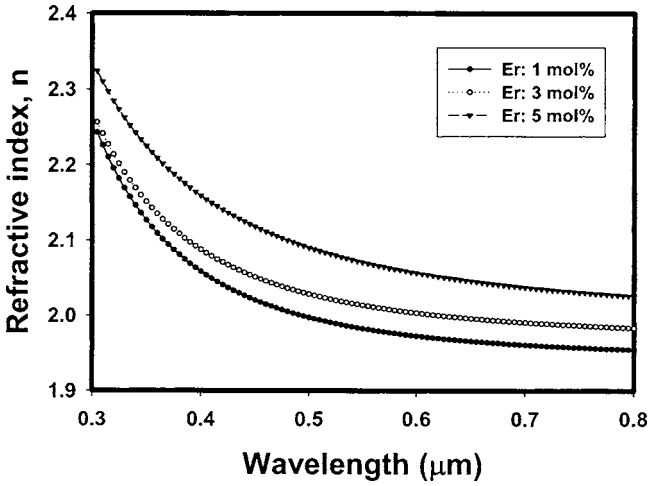

FIG. 3. Refractive index of BST:Er thin films annealed at 700 °C with various Er^{3+} concentrations.

dence, respectively. The refractive index (n) was derived from the ellipsometric parameters and analyzed by a three-phase model. The refractive index of BST:Er films was described using the Cauchy dispersion model, given by

$$n(\lambda) = A + \frac{B}{\lambda^2} + \frac{C}{\lambda^4}, \tag{2}$$

where the parameters A, B, and C are determined from fits to the experimental spectra. The evaluated optical constant n of the BST:Er films is shown in Fig. 3. From the figure, we found that the index of refraction increase slightly as the Er^{3+}-dopant concentration increase from 1 to 5 mol %. It has been known that the BO_6 octahedron significantly governs the optical properties, and other ions in the ABO_3 structure have only a small effect on the optical properties.[31] Although the Er^{3+} ion is likely to take the position of (Ba^{2+}, Sr^{2+}) due to similar ionic radius rather than that of Ti^{4+}, we might attribute the increase of refractive index with increasing Er^{3+} doping to the changes of the electronic polarizability.

Figure 4 shows the room-temperature PL spectra of $Ba_{0.7}Sr_{0.3}TiO_3$ films doped with 3 mol % of Er annealed at 600, 700, 800, and 900 °C. The green peaks at 530 and 550 nm are attributed to the Er^{3+} inner shell $4f\ ^2H_{11/2}$ and $^4S_{3/2}$ to the $^{15}I_{15/2}$ ground level, respectively. In addition, the weak red emission centered at 660 nm is ascribed to the $^4F_{9/2} \rightarrow {}^{15}I_{15/2}$. At the annealing temperature of 600 °C, there are only few broad peaks in the main emission wavelength. When the annealing temperature is above 700 °C, the 550 nm emission peak becomes sharper and splits into several fine peaks attributed to the Stark splitting of the degenerate $4f$ levels under the crystalline field. For BST:Er films annealed at 600 °C, the weak emission intensity and broad spectrum indicated the films possess worse crystallinity, which is consistent with the XRD analysis.

For the 3 mol % Er^{3+}-doped BST films annealed at 700 °C, the excitation-dependent PL spectra are shown in Fig. 5(a). It indicated that these emission peaks do not show any apparent shift with the change in excitation power. In addition, the integrated green emission intensity as a function of excitation power has been plotted in Fig. 5(b) in log–log scale. The integrated PL intensity has a nearly linear dependence on the excitation power. This result confirms that green emission belongs to a one-photon interband transition and no other nonradiative mechanism or nonlinear processes developed from the high excitation condition.

Figure 6 shows the integrated green emission intensities of the BST films doped with various molar ratios of Er at different annealing temperatures of 600, 700, 800, and 900 °C. Obviously, the PL emission at 550 nm reaches its maximum at 700 °C and the emission was partially quenched for other annealing temperatures. The quenching of the green emission has occurred in the BST:Er films, which is directly related to microstructural changes caused by the crystallinity. According to the results of XRD measurements, the crystallization occurred at 700 °C and other formation phase $(Er_2Si_2O_7, Er_2Ti_2O_7)$ forms above this tem-

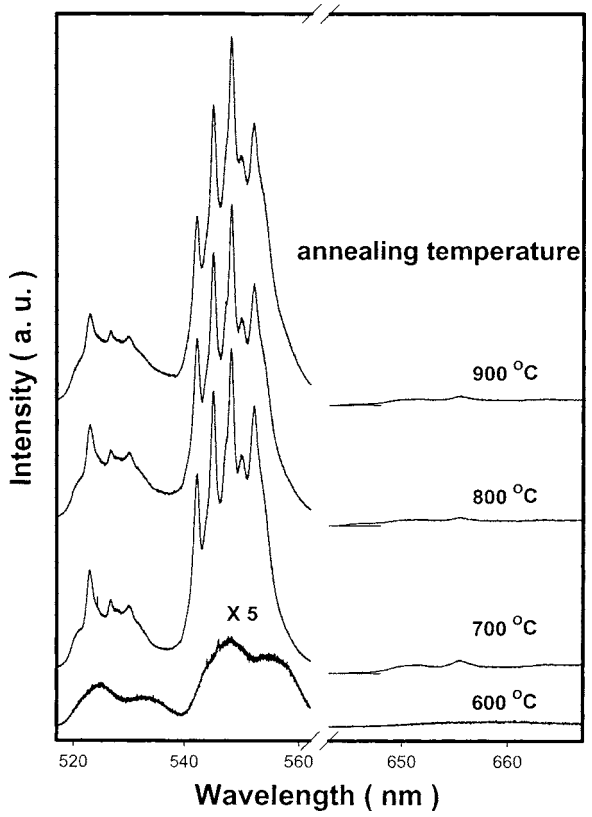

FIG. 4. Room temperature photoluminescence spectra of BST thin films doped with 3 mol % Er under various annealing temperatures. Appropriate offset has been made to highlight the variations in the line shapes of PL spectra.

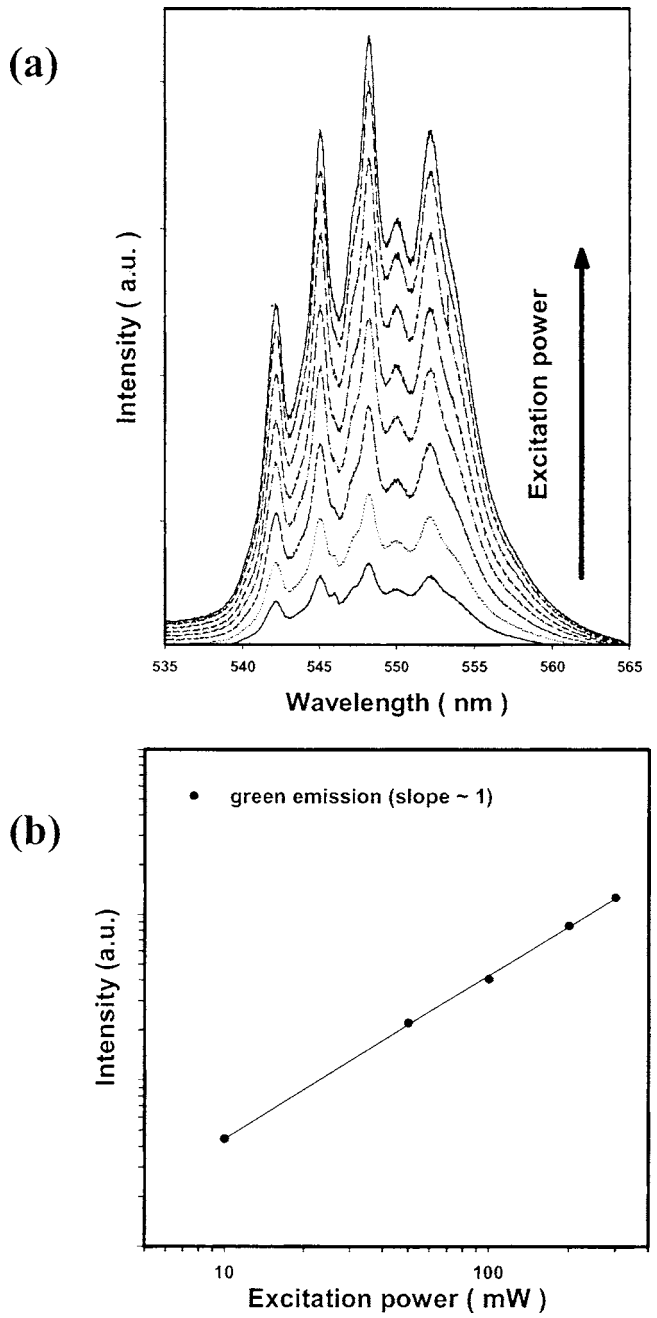

FIG. 5. (a) Excitation-dependent photoluminescence spectra of BST:Er thin film. The arrow indicates the direction of adding excitation power. (b) Integrated intensities of green emission vs the excitation power.

perature. When the BST:Er films are amorphous, the emission intensity depends on the Er^{3+} concentration, as can be seen in Fig. 6. In addition, as the films annealed at 700, 800, and 900 °C, the spectrum is dominated by a main green emission around 550 nm, and we can observe that the emission intensity of the BST:Er film increases as the doping concentration of Er changing from 1 to 3 mol %. When the Er doping concentration exceeds 3 mol %, the PL intensity diminishes. The concentration dependence of the films in the amorphous phase can be explained because the emission intensity is proportional to the solubility of Er in the amorphous matrix. Meanwhile, the presence of clusters in the polycrystalline phase BST:Er films due to high Er concentration will decrease the luminescence efficiency by energy transfer processes due to ion–ion interactions. As shown in Fig. 6, the Er-doped BST thin film with 3 mol % of Er dopants has the strongest PL intensity, while the PL intensity decreased greatly for the Er-doped BST thin film containing 5 mol % Er. The quenching mechanism is thought to be a cross-relaxation process between two closely placed Er^{3+} ions.[32] Very efficient cross relaxation can occur when two or more ions are sited closely together or form a pair or cluster, which results in almost immediate interaction between the ions. The short distance between ions results in enhanced luminescence quenching probability. Accordingly, the emission intensity degrades while the Er concentration exceeds 3 mol %. The mean distances between Er^{3+} ions of the BST films doped with various erbium concentrations are 1.2, 0.8, and 0.7 nm for 1, 3, and 5 mol % Er.[33]

Next, we will focus on the relationship between the crystallinity and emission intensity. In Fig. 6, the emission intensity of the BST film doped with 3 mol % has a maximum value at the annealing temperature of 700 °C. Furthermore, the decrease in luminescence intensity is observed when the annealing temperature is above 700 °C. From the XRD data, we have concluded that the films annealed at 600 °C are amorphous and are polycrystalline when annealed at 700 °C.

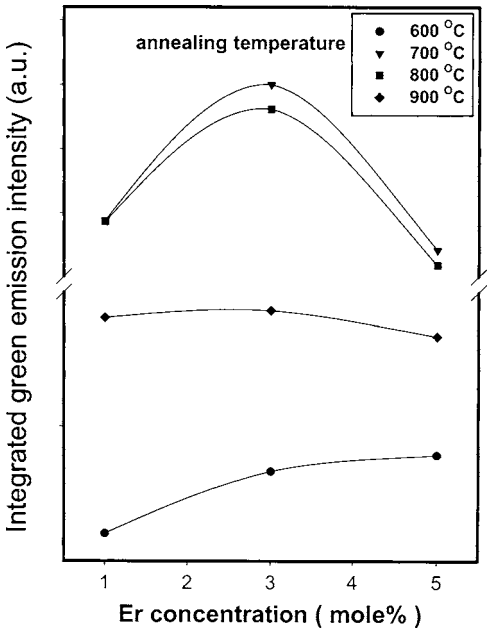

FIG. 6. Integrated green emission intensities of BST:Er thin films as a function of Er concentration and annealing temperatures.

When the films are amorphous, the luminescence efficiency will be low due to the lower degree of crystallization and higher defect density. By increasing the annealing temperature to 700 °C, the green emission becomes stronger than those annealed at 600 °C. In light of the XRD results, it implicitly indicates that the improvement of the crystallinity will enhance the luminescence efficiency. However, the emission intensities decrease while the annealing temperature is above 700 °C. The quenching mechanism of the emission intensity may arise from the formation of other phases and crystal field as described in earlier literature.

IV. CONCLUSION

In conclusion, $Ba_{0.7}Sr_{0.3}TiO_3$ (BST) ferroelectric thin films with various erbium concentrations were grown by the sol–gel method. The crystallization of the films strongly depends on the annealing temperature and dopant concentration. The effects of Er^{3+} concentration on the refractive index of BST thin films have been studied by spectroscopic ellipsometry in the visible region, and a three-phase fitting model was employed to describe the dispersion relation. Our studies show that the index of refraction increase slightly as the Er^{3+}-dopant concentration increases from 1 to 5 mol %. Furthermore, we also found that the addition of Er dopant does not deteriorate the dielectric properties of BST. Photoluminescence measurements indicated that the green band emission intensities vary with various Er concentrations and annealing temperatures. The emission efficiency of BST:Er thin films was found to be dominated by the mean distance between Er^{3+} ions and solubility of Er in polycrystalline and amorphous phases, respectively. With the doping of Er 3 mol %, the emission intensities of the films reach its maximum at an annealing temperature of 700 °C. While the Er concentration exceeds 3 mol %, the emission intensity diminishes due to the presence of clusters. Moreover, the improvement of the crystallinity of BST:Er films also results in the green emission enhancement.

[1]U. Hömmerich, E. E. Nyein, D. S. Lee, J. Heikenfeld, A. J. Steckl, and J. M. Zavada, Mater. Sci. Eng., B **105**, 91 (2003).
[2]D. M. Gill, G. M. Ford, B. A. Block, S. S. Kim, B. W. Wessels, and S. T. Ho, Thin Solid Films **365**, 126 (2000).
[3]H. X. Zhang, C. H. Kam, Y. Zhou, X. Q. Han, S. Buddhudu, and Y. L. Lam, Opt. Mater. (Amsterdam, Neth.) **15**, 47 (2000).
[4]P. A. Tanner, P. T. Law, and L. Fu, Phys. Status Solidi A **199**, 403 (2003).
[5]J. Heikenfeld, M. Garter, D. S. Lee, R. Birkhahn, and A. J. Steckl, Appl. Phys. Lett. **75**, 1189 (1999).
[6]H. X. Zhang, C. H. Kam, Y. Zhou, X. Q. Han, S. Buddhudu, Q. Xiang, Y. L. Lam, and Y. C. Chan, Appl. Phys. Lett. **77**, 609 (2000).
[7]S. M. Takahashi, M. Kanno, and R. Kawamoto, Appl. Phys. Lett. **65**, 1874 (1994).
[8]J. Heikenfeld, D. S. Lee, M. Garter, R. Birkhahn, and A. J. Steckl, Appl. Phys. Lett. **76**, 1365 (2000).
[9]D. Kumar, J. Sankar, K. G. Cho, V. Cracium, and R. K. Singh, Appl. Phys. Lett. **77**, 2518 (2000).
[10]W. Chen, R. Sammynaiken, and Y. Huang, J. Appl. Phys. **88**, 1424 (2000).
[11]G. S. Pomerenke, P. B. Klein, D. W. Langer, Mater. Res. Soc. Symp. Proc. **301**, XXX (1993).
[12]P. L. Thee, Y. K. Yeo, R. L. Hengehold, and G. S. Pomrenke, J. Appl. Phys. **78**, 4651 (1995).
[13]B. A. Block and B. W. Wessels, Integr. Ferroelectr. **7**, 25 (1995).
[14]D. M. Gill, C. W. Conrad, G. Ford, B. W. Wessels, and S. T. Ho, Appl. Phys. Lett. **71**, 1783 (1997).
[15]B. S. Kwak, K. Zhang, E. P. Boyd, A. Erbil, and B. J. Wilkens, J. Appl. Phys. **69**, 767 (1991).
[16]S. Kim, S. Hishita, Y. M. Kang, and S. Baik, J. Appl. Phys. **78**, 5604 (1995).
[17]K. Iijima, T. Terashima, K. Yamamoto, K. Hirata, and Y. Bando, Appl. Phys. Lett. **56**, 527 (1990).
[18]R. A. McKee, F. J. Walker, J. R. Conner, E. D. Specht, and D. E. Zelmon, Appl. Phys. Lett. **59**, 782 (1991).
[19]B. Lee and J. Zhang, Thin Solid Films **388**, 107 (2001).
[20]K. Nashimoto, D. K. Fork, F. A. Ponce, and J. C. Tramontana, Jpn. J. Appl. Phys., Part 1 **32**, 4099 (1993).
[21]T.-J. Zhang, H. Ni, and W. Wang, J. Mater. Synth. Process. **10**, 17 (2002).
[22]C. L. Jia, K. Urban, S. Hoffmann, and R. Waser, J. Mater. Res. **13**, 2206 (1998).
[23]S. Hoffmann and R. Waser, J. Eur. Ceram. Soc. **19**, 1339 (1999).
[24]K. Hafidi, Y. Ijdiyaou, M. Azizan, E. L. Ameziane, A. Outzourhit, T. A. Nguyen Tan, M. Brunel, Appl. Surf. Sci. **108**, 251 (1997).
[25]J. H. Hwang, S. K. Choi, and Y. H. Han, Jpn. J. Appl. Phys., Part 1 **40**, 4952 (2001).
[26]J. H. Hwang and Y. H. Han, Jpn. J. Appl. Phys., Part 1 **40**, 676 (2001).
[27]C. B. Samantaray, A. Dhar, D. Bhattacharya, M. L. Mukherjee, and S. K. Ray, J. Mater. Sci.: Mater. Electron. **12**, 365 (2001).
[28]R. Naik *et al.*, Phys. Rev. B **61**, 11367 (2000).
[29]C. L. Li, Z. H. Chen, Y. L. Zhou, H. B. Lu, C. Dong, F. Wu, and H. Chen, J. Appl. Phys. **86**, 4555 (1999).
[30]R. M. A. Azzam and N. M. Bashara, *Ellipsometry and Polarized Light* (North-Holland, Amsterdam, 1977).
[31]K. Y. Chan, W. S. Tsang, C. L. Mak, K. H. Wong, and P. M. Hui, Phys. Rev. B **68**, 144111 (2002).
[32]W. J. Miniscalco, J. Lightwave Technol. **9**, 234 (1991).
[33]C. Y. Chen, R. R. Petrin, D. C. Yeh, W. A. Sibley, and J. L. Adam, Opt. Lett. **14**, 432 (1989).